In vivo and Cellular Trafficking of Acetalated Dextran Microparticles for Delivery of a Host-Directed Therapy for *Salmonella enterica* Serovar Typhi Infection

Monica M. Johnson[a], Michael A. Collier[a], Ky V. Hoang[b], Erica N. Pino[a], Elizabeth G. Gurysh[a], Matthew D. Gallovic[a], Md. Shamim Hasan Zahid[a], Naihan Chen[a], Larry S. Schlesinger[b], John S. Gunn[c], Eric M. Bachelder[a], and Kristy M. Ainslie[a,d,*]

[a]Division of Pharmacoengineering and Molecular Pharmaceutics, Eshelman School of Pharmacy, University of North Carolina-Chapel Hill, Chapel Hill, NC 27599, USA

[b]Texas Biomedical Research Institute, San Antonio, TX 78227, USA

[c]Department of Microbial Infection and Immunity, The Ohio State University, Columbus, OH 43210, USA

[d]Department of Microbiology and Immunology, University of North Carolina-Chapel Hill, Chapel Hill, NC 27599, USA

Abstract

Previously we have encapsulated host-directed therapy AR-12 into acetalated dextran (Ace-DEX) microparticles (MPs) to mitigate drug toxicity and passively target phagocytic host cells. Herein, we have improved upon our initial emulsion-based formulation of Ace-DEX MPs encapsulating AR-12 (AR-12/MPs) by improving the drug encapsulation efficiency, evaluating sterilization processes for manufacturing, and understanding cellular and *in vivo* trafficking of the MPs. By using an alternative solvent system, ethyl acetate, we report an increased encapsulation efficiency of AR-12 while maintaining the pH-responsive degradation kinetics of Ace-DEX MPs. To better manufacture this novel antimicrobial formulation, we sterilized AR-12/MPs by gamma irradiation or ethylene oxide and evaluated their efficacy against intracellular *Salmonella enterica* serovar Typhi. Sterilized AR-12/MPs resulted in a significant reduction in intracellular bacterial burden compared to Blank/MPs. We also characterized intracellular trafficking of Ace-DEX MPs encapsulating fluorophores, which demonstrated internalization of MPs in endo/lysosomal compartments and time and degradation-rate dependent lysosomal escape into cytosolic compartments. Additionally, *in vivo* toxicity was mitigated following encapsulation of AR-12, where the maximum tolerated dose of AR-12 was increased compared to soluble treatment via intranasal, intravenous, and intraperitoneal administration routes. Following *in vivo* trafficking of

*Corresponding author: Kristy Ainslie: ainsliek@email.unc.edu. 125 Mason Farm Road, 4211 Marsico Hall, CB #7362, Chapel Hill, NC 27599, USA.

Ace-DEX MPs via the same routes, intranasal administration demonstrated the highest accumulation in the lungs, liver and kidneys, which persisted out to 240 hours. Overall, we have advanced the formulation of this host-directed therapy and broadened the understanding of Ace-DEX MP delivery.

Graphiacl Abstract
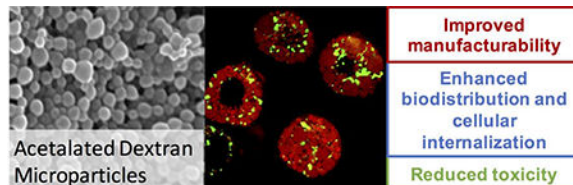
Introduction

Host-directed therapeutics (HDTs) offer a means to circumvent resistance mechanisms by targeting the host cell rather than the pathogen[1]. This is thought to not only overcome multi-drug resistant pathogens, but also limit the emergence of additional drug-resistance by eliminating selective pressure on the pathogens [2, 3]. A novel HDT with the potential to clear intracellular pathogens is AR-12 (also known as OSU-03012), an IND-approved derivative of celecoxib that lacks cyclooxygenase-2 inhibitor activity. AR-12 has been reported to enhance host-directed eradication of numerous intracellular infectious agents via several proposed mechanisms including the repression of the host cell chaperone machinery, inhibition of kinase pathways, and up-regulation of autophagy [4–10]. Due to the hydrophobic nature of AR-12, studies show that cellular internalization of soluble AR-12 is an inefficient process [4]. Additionally, AR-12 is cytotoxic to the host cell at concentrations of $\times 7$ μM, which limits the therapeutic range that can be explored [4].

To improve the solubility and mitigate AR-12's toxicity, we developed a carrier system comprised of a modified polysaccharide, acetalated dextran (Ace-DEX), which couples the strengths of both a biodegradable and pH-responsive polymeric drug delivery vehicle and has demonstrated promising results when formulated into MPs [11]. Ace-DEX is chemically modified by forming cyclic and acyclic acetal groups on the reactive hydroxyl groups of dextran, rendering the biomaterial organic soluble and acid-labile [12, 13]. By altering the reaction times, Ace-DEX can be synthesized with highly tunable degradation kinetics and formulated into MPs that can encapsulate small molecules and proteins with physicochemically distinct properties [14, 15]. Importantly, the size (200–1000 nm) and pH-dependent degradation of Ace-DEX MPs enables passive targeting of phagocytic cells. Once internalized, the low pH environments within phagocytic cells results in rapid degradation over a period of hours to days within the low pH endo/lysosome, in contrast to sustained degradation over a period of weeks to months at physiological pH [12–15]. Other biodegradable polymers, such as poly lactic-co-glycolic acid (PLGA), have minimal pH sensitivity, generate acidic by-products that can be cytotoxic to the host cell, and therefore are not optimal for tunable intracellular drug release [16–18]. Additionally, Ace-DEX is known

to protect encapsulated cargo outside of the cold-chain, potentially increasing treatment accessibility worldwide [19].

Due to the unique nature of intracellular infectious agents, the conventional therapeutic approach (e.g. systemic delivery of soluble drug) could significantly benefit from a controlled release system that passively targets intracellular sites of infection. Previously, we have shown *in vitro* that formulating AR-12 into Ace-DEX MPs (AR-12/MPs) increases intracellular drug concentrations while also reducing host cytotoxicity in several cell lines including murine bone marrow-derived macrophages and human monocyte-derived macrophages when compared to soluble AR-12 treatment [4]. Additionally, dose sparing was observed in treatment of intracellular *Salmonella enterica* serovar Typhimurium and *Francisella tularensis*, and when combined with conventional therapy, a significantly greater reduction in bacterial burden was observed [4, 20].

While all of these findings show great promise for AR-12/MPs as a HDT, some of the shortcomings of the formulation needed to be addressed. Therefore, the current study investigates the improved formulation and manufacturability of AR-12/MPs by altering solvent systems for increased encapsulation efficiencies and evaluating various sterilization techniques. Using the improved AR-12/MP formulation, treatment of intracellular *S.* Typhi was evaluated to assess if sterilization altered therapeutic efficacy.

In addition to improved MP formulation, pharmacological and toxicological outcomes were also assessed. Studies have observed that a majority of internalized drug carrier systems often become trapped in endo/lysosomal vesicles and cargos degraded before they reach their desired intracellular target, significantly impacting therapeutic efficacy [21]. Therefore, we aimed to evaluate the intracellular delivery and pH-responsive degradation kinetics of Ace-DEX MPs, allowing us to better tune the delivery platform for controlled release to therapeutic sites of action. This is important for treatment of facultative intracellular pathogens such as *Francisella* and *Salmonella*, which are inherently difficult to treat because they reside in intracellular vesicles, requiring therapeutic delivery to these cytosolic compartments. Additionally, temporal dissemination and bacteremia of said pathogens is highly dependent on the route of infection, and a potential dictator of effective therapy [22]. Therefore, we evaluated the systemic delivery of Ace-DEX MPs by common routes of administration (intranasal, intravenous, and intraperitoneal) to investigate the biodistribution and organ-specific accumulation, specifically at the sites of infection such as liver, spleen, and lung. To further evaluate the pre-clinical potential of AR-12 encapsulated Ace-DEX MPs, the maximum tolerated dose (MTD) following the same routes of administration was evaluated to determine if AR-12 toxicity could be mitigated by encapsulation. Toxicity studies, such as MTD, are a crucial step in evaluating the clinical translation of the controlled release formulation, as other polymeric delivery platforms have failed to progress beyond pre-clinical evaluation due to *in vivo* toxicity concerns, possibly by their inability to release therapeutic payload at the optimal dosing range [23]. Together, this study evaluated the manufacturability, efficacy, organismal trafficking, and reduced toxicity of Ace-DEX MPs encapsulating AR-12 as a novel HDT for treatment against intracellular pathogens.

Materials and Methods

Chemicals

All products were purchased from Sigma (St. Louis, MO) unless otherwise stated. Texas Red-conjugated dextran, LysoTracker Red, and LysoTracker Green were purchased from ThermoFisher-Scientific (Waltham, MA). Indocyanine green (ICG) was purchased from VWR (Radnor, PA). AR-12 was from Arno Therapeutics (Flemington, NJ, USA). Water was purified using a Millipore (Billerica, MA, USA) Milli-Q Integral water purification system. Fluorescence and absorbance measurements were obtained with a Molecular Devices (Sunnyvale, CA, USA) Spectra Max M2 plate reader.

Cell culture

Femoral bones isolated from 6–8 week old male and female BALB/c mice were used for progenitor cell isolation. Bone marrow progenitor cells (pooled from 2 mice) were cultured in DMEM media supplemented with 15% L929 cell supernatant that contains granulocyte-macrophage colony stimulated factor (GM-CSF) for 7 days until fully differentiated into bone marrow-derived macrophages (BMDMs). Human monocyte-derived macrophages (hMDMs) were isolated from the blood of healthy donors following protocols approved by the Ohio State University Institutional Review Board, as previously reported [4]. Cells were maintained in a humidified incubator with 5% CO_2 at 37 °C. In addition to GM-CSF, filtered DMEM media also contained 10% fetal bovine serum (FBS), 100 μg/mL streptomycin and 100 U/mL penicillin, except during infections. All animal procedures were approved and conducted in accordance with the National Institutes of Health guidelines and approved by the University of North Carolina at Chapel Hill Institutional Animal Care and Use Committee.

Synthesis of acetated dextran (Ace-DEX) polymer and characterization by NMR

Ace-DEX was synthesized as previously described by Kauffman et al.[13]. Native or Texas Red-conjugated dextran (71 kDa) was reacted with 2-ethoxypropene (Brookview Scientific, Carmel, IN) under acid catalysis for a period of time to form cyclic and acyclic acetals, the ratio of which was determined by ^{1}H nuclear magnetic resonance (NMR) spectrometry. The reaction times were 5 and 30 min, which resulted in relative cyclic acetal coverages (CAC) of 26% and 55%, respectively.

Fabrication of AR-12, FITC-BSA, ICG, or Texas Red/Ace-DEX microparticles (MPs) by ultrasonication and solvent evaporation

Ace-DEX MPs were generated by a single or double oil-in-water emulsion ultrasonication technique as previously described [12]. Briefly, Ace-DEX at 26% and 55% CAC was combined at various weight loadings (% w/w) with either AR-12, fluorescein isothiocyanate-bovine serum albumin (FITC-BSA) or ICG (only 55%) and dissolved in ethyl acetate (EA) or dichloromethane (DCM). To this solution, polyvinyl alcohol (PVA) (3% wt/wt in 1X phosphate buffered saline [PBS]) was added and the mixture was sonicated on ice using a Misonix Ultrasonic Liquid Processor (Farmingdale, NY; 60 W, duty cycle 50%). The emulsion was hardened in 0.3% PVA in PBS and stirred for 3 hours to allow

evaporation of the organic solvent. To remove un-encapsulated drug, the solution was centrifuged and washed in basic water (0.04% v/v triethylamine) prior to freezing and lyophilization. To create blank MPs, the same procedure was used without the addition of drugs.

Texas Red-conjugated Ace-DEX microparticles (TR/MPs) were fabricated using the same protocol as above, but with a blend of 10% Texas Red conjugated Ace-DEX and 90% native Ace-DEX polymer. Rather than freezing and lyophilizing, TR/MPs were suspended in media and used immediately following the wash steps. To prevent endotoxin contamination, all dishes and glassware were soaked in 1.0M sodium hydroxide overnight, washed with acetone, and dried before use. Prior to use, both loaded MPs and empty MPs were confirmed to have endotoxin levels below FDA guidelines (0.00025 endotoxin units per mg) by a Pierce Chromogenic LAL Endotoxin Assay Kit (Thermo Fisher), performed according to the manufacturer's instructions.

Sterilization of AR-12/MPs

Formulated AR-12/MPs were sterilized by either gamma irradiation or ethylene oxide treatment. For gamma irradiation, particles were placed on dry ice and subjected to gamma irradiation at a dose of 2.2 Gy/min for a total dose of 8.5 kGy (Model Mark I-68; J.L collimator, ^{137}Cesium γ-ray source, Shepherd & Associates, San Fernando, CA). Sterilization of AR-12/MPs by ethylene oxide was performed at Anderson Products (Haw River, NC, USA).

Size, imaging, and encapsulation efficiencies of AR-12/MPS, FITC-BSA/MPs and ICG/MPs

Hydrodynamic size of MPs was determined by dynamic light scattering (DLS; Brookhaven) at 0.1 mg/mL in basic water. AR-12/MPs, TR/MPs, FITC-BSA/MPs, and ICG/MPs were imaged using scanning electron microscopy (SEM) located at the Chapel Hill Analytical and Nanofabrication Laboratory (Hitachi S-4700 Cold Cathode Field SEM). SEM images were used to confirm DLS size and polydispersity results, and to ensure all un-encapsulated drug was removed during washing. Encapsulation efficiency (EE) was determined by preparing a 1 mg/mL solution of AR-12/MPs, FITC-BSA/MPs or ICG/MPs in DMSO alongside a standard curve of un-encapsulated drugs dissolved in DMSO. The samples were read on a plate reader using fluorescence for: AR-12 ($\lambda_{ex}/\lambda_{em}$ 280/380nm), FITC ($\lambda_{ex}/\lambda_{em}$: 496/590nm), or ICG ($\lambda_{ex}/\lambda_{em}$: 788/813nm). The fluorescence was calculated using regression analysis of the un-encapsulated fluorophore standard curves.

Release kinetics of AR-12/MPs, FITC-BSA/MPs and ICG/MPs

AR-12/MPs (non-sterilized and sterilized), FITC-BSA/MPs, and ICG/MPs (n= 3) were suspended at a concentration of 0.5 mg/mL in either PBS to mimic physiological pH (pH 7.4) or 0.3M sodium acetate to mimic the acidic pH of endo/lysosomal compartments (pH 5.0) and placed in a shaking heat block at 37 °C. After set time-points, the MPs were centrifuged (Thermo Fisher) at $21,000 \times g$ for 10 minutes and the supernatant and pellets were individually frozen. Once all time points had been collected, the sample supernatants were read on a plate reader as described above and the percent of AR-12, FITC-BSA, or ICG retained within the MPs at each time point was calculated.

Degradation of sterilized AR-12/MPs

To determine if particle sterilization affected the particle degradation rate, degradation studies were performed for sterilized and non-sterilized AR-12/MPs and Blank Ace-DEX MPs, as previously described [15, 24]. Particles were re-suspended at a concentration of 1.5 mg/mL in either PBS (pH = 7.4) or 0.3 M sodium acetate buffer (pH 5.0). Samples were agitated on a shaker plate (150 rpm) at 37 °C. At predetermined time points, the solution was vortexed, and its absorbance was read at 600 nm. The degradation profile of MPs was determined by comparing their absorbance values at different time points to the recorded absorbance at 0 hours. The percent degradation of each sample is equal to the difference between its absorbance reading at the specified time point and that at 0 hours, divided by the absorbance reading at 0 hours.

Efficacy of Sterilized AR-12/MPs against intracellular *Salmonella* enterica serovar Typhi infection *in vitro*

Wild-type *Salmonella enterica* serovar Typhi (TY2)-infected hMDMs were treated with sterilized AR-12/MPs, as previously described [4]. Overnight cultures of *S.* Typhi were prepared for infection of hMDMs by sub-culture (1:50) in fresh Luria-Bertani broth (LB; Difco, Detroit, MI, USA) broth and incubated for 4 hours at 37°C. Bacteria were then collected by centrifugation at $3,000 \times g$ for 10 minutes and suspended in PBS to an optical density of 0.6 at 600nm, which was equivalent to $\times 5 \times 10^8$ CFUmL^{-1}. hMDMs were infected with *S.* Typhi at a multiplicity of infection (MOI) of 20:1 in the presence of 2% autologous serum in RPMI 1640 (Gibco-Life Technologies). Two hours after infection, extracellular bacteria were removed by adding gentamicin (100 μg/mL) to the culture medium for 1 hour, followed by thoroughly washing the cell layer three times with pre-warmed RPMI 1640. Infected hMDMs were then treated with sterilized or non-sterilized AR-12/MPs (5 μM) and respective Blank MPs in fresh culture medium. Gentamicin was also added at 10 μg/mL to eliminate potential re-infection by extracellular bacteria. At 22 hours post-treatment, infected hMDMs were lysed with 0.1% Triton X-100, serially diluted, and spread on LB agar plates. The surviving intracellular bacteria were determined by enumerating CFU after 24 hour incubation at 37°C.

Co-localization and endo/lysosomal escape of TR/MPs and FITC-BSA/MPs by confocal laser scanning microscopy

Bone marrow-derived macrophages (BMDM) cells (5×10^5) were plated on coverslip chamber slides pre-coated with poly-d-lysine (150 μg/mL, 4 hours) to enhance cell adhesion. Cells were incubated with 0.5 mg/mL of either FITC-BSA-encapsulated MPs or TR/ MPs for 16 hours at 37 °C, followed by three washes with serum-free DMEM before replacing media. Soluble FITC-BSA, treated for 8 hours, was used as a positive control. Following a series of incubation periods (1, 2, 3, 4, and 5 days), the cells were washed three times and incubated with organelle-specific contrasting fluorescent dye LysoTracker™ Red or Green (500 nM; Molecular Probes) for 30 min at 37 °C just prior to imaging. The endo/lysosomes appeared red or green in color when labeled with LysoTracker Red or LysoTracker Green and visualized under RFP ($\lambda_{ex}/ \lambda_{em}$: 595/613 nm) or FITC ($\lambda_{ex}/ \lambda_{em}$: 494/ 519 nm) filters, respectively. Live cell imaging was performed using a laser scanning confocal microscope

(Zeiss LSM710, 40× oil, UNC-CH Pathology Core). Z-stack images (0.8 μm in thickness) were taken of the cells using both filters. Differential interference contrast (DIC) confocal images were collected simultaneously with transmitted light by excitation at 488 nm. Sequential rather than simultaneous acquisition was used to avoid bleed-through between the two fluorescent channels. The extent of co-localization between fluorescent particles and endo/lysosomal compartments (LysoTracker™ Red or Green) was quantified using the JACoP plug-in for Image J [13]. The specific algorithm used was based on the Mander's overlap coefficient, which varies from 0 to 1, the former corresponding to non-overlapping images and the latter reflecting 100% co-localization between both images [25].

Semi-quantitative measurement of endo/lysosomal escape induced by Ace-DEX MPs by measuring release of N-acetyl-ß-D-glucosaminidase (ß-NAG)

Cell permeabilization with saponin-containing buffer was developed based off previously reported studies using a similar amphipathic glycoside, digitonin [26, 27]. Initially, the saponin concentration and treatment time was optimized in BMDMs treated with saponin-containing buffer (20, 30, or 40 μg/mL saponin diluted from stock 20 mg/mL in DMSO, 250 mM sucrose, 20mM Hepes, 10mM KCL, 1.5 mM $MgCl_2$, 1mM EDTA, 1mM EGTA, pH 7.4) on ice for 5, 15, and 30 min and analyzed as previously described [26]. Cells lysed with Triton X-100 (0.1 %) were used as 100% lysed positive controls.

BMDMs plated at 2×10^6 cells per well in a 6-well plate were incubated with 26% or 55% CAC blank Ace-DEX MPs (0.5mg/mL) as described above, then incubated for a total of 1 or 5 days. Following incubation, cells were washed three times with PBS, scraped from the plate, and re-suspended in saponin-containing buffer (20 μg/mL saponin) for 30 min. 10 μL of permeabilized cells were removed and stained with 0.02% trypan blue, and counted to ensure >80% of cells were permeabilized. After a series of centrifugation steps to remove membrane components and organelles (10 min at $1000 \times g$, 30 min at $20,000 \times g$), 0.2 mL of supernatant was assessed for enzyme activity using the commercially available N-acetyl-ß-D-glucosaminidase (ß-NAG) assay kit following the manufacturers protocol (Abcam, United Kingdom). Values are expressed as ß-NAG enzyme activity normalized to enzyme activity reported from 100% lysed cells.

Maximum tolerated dose of AR-12/MPs

A traditional 3+3 dose escalation was used to determine the maximum tolerated dose (MTD) of AR-12/MPs [28]. 6–8 week old female BALB/c mice were weighed and assessed before administration to determine baseline weight and activity. Mice ($n = 3$/group) were administered AR-12/MPs, soluble AR-12 dissolved in a soluble vehicle (Poly-ethylene glycol 400, saline, ethanol, 50:35:15), PBS, or soluble vehicle via intranasal, intravenous, or intraperitoneal routes. For intranasal administration, mice were anesthetized via isoflurane inhalation and 10 μL was pipetted into each nostril (for a total of 20 μL) and were held until they regained consciousness. For intravenous administration, 100 μL was injected into the tail vein. For intraperitoneal administrations, 100 μL was injected into the intraperitoneal space. Following administration, mice were weighed and monitored at regular time intervals to ensure their health was not at risk. If a mouse lost more than 15% of its pre-administration body weight, it was determined that the dose was not tolerated, and that mouse was

euthanized immediately. If all three mice survived the dose of AR-12 that was administered, the dose was increased until the dose was not tolerated to determine the MTD.

Trafficking of indocyanine green microparticles (ICG/MPs) *in vivo*

BALB/c mice (female; 6–8 weeks old) were administered 0.5 mg/kg of encapsulated ICG via intranasal, intravenous, or intraperitoneal routes, as described above ($n = 4$/group). At pre-determined time points, mice were euthanized and organs of interest were harvested. Following extraction, organs were aligned and imaged using an In Vivo Imaging System (IVIS, UNC Chapel Hill Biomedical Research Imaging Core) kinetic with appropriate ICG settings and mean fluorescent intensity was reported as arbitrary units (AU).

Statistical analysis

All data were analyzed using GraphPad Prism software. Data are expressed as mean ± standard error of the mean (SEM) and comparison between groups was analyzed using one-way analysis of variance (ANOVA), with differences between groups assessed using Tukey's post hoc test. A $p < 0.05$ was considered statistically significant.

Results and Discussion

Characterization of Ace-DEX MPs encapsulating AR-12 and various fluorophores

The development of new treatment approaches for infections is vital and host-directed therapies are one avenue for drug development. AR-12/MPs demonstrate clear advantages as a host-directed therapeutic vehicle, exhibiting controlled and sustained release for clearance of intracellular pathogens [4, 20, 29]; however, it was hypothesized that modulation of the formulation parameters could increase encapsulation efficiency (EE). Using an emulsion-based technique, Ace-DEX MPs encapsulating AR-12 were fabricated via sonication using either DCM or EA as the organic solvent. Regardless of the solvent, the particles appeared to have similar morphologies and size ranges (Figure 1A and 1B). As measured by DLS, the size of the particles was determined to be 255 ± 45 nm for DCM particles and 260 ± 37 nm for EA particles. The EE was 31.5% for DCM particles and 80.6% for EA particles for 2% by weight initial loading (Table 1). For EA particles, increasing the initial weight loading of AR-12 from 2% by weight up to 20% by weight did not reduce the EE (Table 1). Therefore, we determined that switching the organic solvent from DCM to EA allowed for a much higher EE most likely due to increased solubility of AR-12 in EA. In an emulsion process, the organic soluble components reside within the immiscible organic solvent when the bulk aqueous phase is added. If the drug and/or polymer is not highly soluble within the organic phase, it will diffuse readily into the bulk aqueous phase, lowering the EE [30]. EE is important for clinically applicable formulations, as lower drug loading means higher excipient loads, which can make treatment difficult [31]. EA was used to encapsulate fluorophores in native dextran MPs (indocyanine green (ICG/MPs) or FITC-BSA/MPs) or Texas-Red conjugated dextran MPs (TR/MPs). EE and particle size for these MPs was comparable to the AR-12/MPs, and these values are reported for MPs fabricated from different relative cyclic acetal coverages (%CAC) Ace-DEX to vary degradation rates (Supplemental Figure 1, Supplemental Table 1).

AR-12/MPs release kinetics using different solvents

The ability of AR-12/MPs to retain AR-12 in neutral and acidic environments was analyzed. In a pH 5.0 environment, AR-12 was released quickly from MPs with close to 100% release from both DCM and EA formulations shortly after 24 hours (Figure 2). At pH 7.4, AR-12/MPs formulated using DCM released AR-12 from MPs more quickly than those formulated with EA. After one week in pH 7.4 conditions, roughly 60% of AR-12 was released from the MPs formulated with DCM and approximately 15% of AR-12 was released from the MPs formulated with EA. The improvement in release kinetics by changing the solvent system from DCM to EA most likely stems from AR-12 being more homogenously distributed within the organic phase droplet in the emulsion. Additionally, if AR-12 is less soluble in DCM, it is possible that aggregates of AR-12 form within the organic phase droplet which can lead to faster overall release. Because the Ace-DEX polymer was unchanged in either solvent system, the degradation time was unchanged and thus, the differences are most likely predicated upon solvent-polymer-drug interactions.

Degradation and release kinetics of sterilized AR-12/MPs

An important aspect in clinical translation is evaluating the manufacturability of the drug formulation, specifically the ability to sterilize MPs without altering the biological activity of the drug/cargo. For any clinical production, MP formulations must be either produced and subsequently sterilized, or manufactured within a clean room environment [32]. Of the many processes available for sterilization, gamma irradiation and ethylene oxide treatment were selected for use in the current study because they are the most readily used and cost effective procedures [33]. Following these sterilization techniques, degradation and release kinetics of AR-12/MPs (formulated with EA) was performed in acidic (pH 5.0) and neutral (pH 7.4) environments. In pH 5.0 environments, non-sterilized and sterilized particles have fairly similar degradation and release kinetics (Figure 3 A & 3C, respectively). However, at pH 7.4, both sterilization techniques rendered some differential degradation (Figure 3B) and AR-12 release profiles (Figure 3D), yet it took roughly 400 hours (×2.5 weeks) before these differences became apparent. As evident in Figure 3, gamma irradiated particles had faster release and degradation rates than ethylene oxide and non-sterilized particles. Additionally, we have previously demonstrated effective sterilization of Ace-DEX MPs by gamma irradiation in which particles were streaked on agar plates and no bacteria growth was observed[34]. Therefore, these studies determine that AR-12/MPs can be sterilized by multiple techniques without loss in acid-sensitivity, which is an important parameter for any clinical progression of the formulation.

Efficacy of Sterilized AR-12/MPs against *S.* Typhi

AR-12/MPs were evaluated for their activity against the intracellular pathogen *S.* Typhi, to ensure sterilization did not alter therapeutic efficacy of AR-12 as a host-directed antimicrobial agent. This work continues our previous study which reports a more in-depth analysis of AR-12/MPs as a therapy for *S.* Typhi infection [4]. Human monocyte-derived macrophages (hMDMs) were infected with *S.* Typhi and then treated with sterilized or non-sterilized AR-12/MPs (Figure 4). Following treatment with either non-sterilized AR-12/MPs or gamma irradiated AR-12/MPs, a significant reduction in intracellular bacterial burden

was observed. While not significant relative to blank controls (Blank MPs), a similar trend was also observed following ethylene oxide-treated AR-12/MPs. However, the reduced bacterial burden observed in blank ethylene oxide-treated MPs suggests that the sterilization may alter Ace-DEX slightly. Ethylene oxide treatment results varied results with other biomaterials, with biological effects. It lead to aggregation of poly(D,L)lactide microspheres [35] and poly(lactic-co-glycolic) acid (PLGA) MPs, the later resulting in increased accumulation and inflammation at sites of injection *in vivo*[36]. Together, these results indicate that sterilization of MPs by gamma irradiation did not result in altered therapeutic efficacy against an intracellular infection. Also, they are consistent with our previous study demonstrating that bioactivity of encapsulated cargo in Ace-DEX MPs was not altered following sterilization by gamma irradiation [34]. This is important to note, since various sterilization techniques have been shown to inhibit the activity of the drug delivery cargo [37]. Taken together, these results further validate the utility of Ace-DEX as a carrier vehicle.

Cellular uptake, intracellular trafficking, and endo/lysosomal escape of Texas Red/MPs and FITC-BSA/MPs

A limiting step for achieving effective therapy against intracellular pathogens is to facilitate endo/lysosomal escape and ensure cytosolic delivery of the potential therapeutic. Herein, we evaluated the intracellular trafficking of Ace-DEX MPs and endosomal escape of encapsulated cargo in murine bone marrow-derived macrophages (BMDMs) at 1, 3, and 5 days post treatment (Figure 5). These later time-points were chosen to highlight the tunability of the Ace-DEX MP platform and the controlled release of encapsulated cargo out to 5 days post treatment. Live cell confocal microscopy was performed to detail intracellular trafficking, and co-localization with endo/lysosomes was visualized in contrast with a commercially available ionophore, LysoTracker Green. Following treatment with TR/MPs, MPs are readily taken up into the endo/lysosomal compartments, as observed by a punctate expression and co-localization with LysoTracker Green at 1 day post treatment (Figure 5). We also observed this as early as 5 hours post treatment (Supplemental Figure 3). A steady time-dependent decrease in both co-localization with lysosomes and Texas Red (TR) fluorescent intensity was observed out to 5 days, potentially indicating MP degradation in the low pH environment. Co-localization with LysoTracker Green was confirmed using Manders Overlap Coefficient (equation 1), with >0.5 overlap consistent with co-localization (Figure 5B). At 3 days post exposure, a similar punctate expression was observed, however, the merged image demonstrates diffuse TR fluorescence in non-endo/lysosomal compartments, indicating endo/lysosomal leakage. At 5 days post exposure, almost no co-localization was observed in addition to reduced TR fluorescence throughout the cell, likely resulting from MP degradation and diffusion of TR dextran at longer incubation periods. These results indicate that MPs are readily taken up into the cellular and co-localize within lysosomal compartments, followed by MP degradation in the low pH environment resulting in lysosomal escape. A similar study evaluating trafficking using PLGA MPs also observed rapid uptake as early as 4 hours post treatment, however, the study failed to track MP intracellular co-localization beyond the initial time-point [26]. Other studies utilizing acid-sensitive biomaterials such as poly (beta-amino) esters also demonstrated cytosolic delivery; however, these polymeric drug delivery platforms are difficult to synthesize, lack the

tunability inherent to Ace-DEX, and demonstrate rapid degradation and burst release shortly after treatment (4–6 hours) [37], which is not ideal for sustained delivery applications.

We next sought to investigate the tunability of our delivery system by altering the reaction times during Ace-DEX synthesis to formulate fast- and slow-degrading MPs (26% and 55% CAC, respectively). The release profiles between the two formulations are strikingly different; the fast-degrading MPs releasing encapsulated cargo within hours in a low pH environment, while the slow-degrading particles demonstrated a much slower time-dependent release out to 24–72 hours (Supplemental Figure 2). Treatment of BMDMs with fast- and slow-degrading Ace-DEX MPs (Figure 6A and 6B, respectively) encapsulating a large, hydrophilic protein (FITC-BSA) demonstrated rapid uptake at 1 day post treatment, with a punctate expression pattern indicative of vesicular localization, which is in stark contrast to the encapsulated (i.e. soluble) FITC-BSA treatment after only five hours (Figure 6). Co-localization with Lysotracker Red was clearly visible, and confirmed using Manders Overlap Coefficient (Figure 6C). Consistent with the release studies, co-localization at 3 and 5 days post treatment was significantly different between the fast- and slow-degrading particles, indicating that Ace-DEX particles are tuned to release their cargo at CAC-dependent rates upon degradation in the low pH environment of the endo/lysosome. Previous studies in our laboratory have also demonstrated CAC-and pH-dependent intracellular release of encapsulated cargo from Ace-DEX MPs in bone marrow-derived dendritic cells [38]. The pH-responsive intracellular release is a key attribute for clinically relevant drug delivery formulations, since it provides spatiotemporal control of therapeutic delivery and minimizes destruction of therapeutic molecules [39]. Additionally, it is important to note that both MP formulations demonstrated significantly higher co-localization with endo/lysosomes and extended internalization of cargo compared to soluble FITC-BSA, highlighting the controlled intracellular delivery kinetics by MP encapsulation. Although these studies infer that the encapsulated cargo is released from the endo/lysosome, there was low FITC-BSA fluorescence observed in the cytosol even out to 5 days following treatment of the slow-degrading MPs. This was likely due to slower MP degradation kinetics that proceeded beyond 5 days, or limited cytosolic diffusion of the larger molecular weight of FITC-BSA molecules. Since previous studies demonstrating that Ace-DEX MPs encapsulating AR-12 are capable of passively targeting phagocytes and inducing autophagy in *S.* Typhi infected cells[4], these results confirm the feasibility of Ace-DEX MPs for delivering a host-directed therapy for intracellular infections.

ß-NAG assay to evaluate endo/lysosomal escape by Ace-DEX MPs

Although quantitative assessment of microscopic images provides one approach for studying the distribution of cargos among the cytosolic space and endo/lysosomal compartments, a semi-quantitative method was then used to quantify the endo/lysosomal escape of cargos induced by Ace-DEX MPs. This method was adapted from Zhan et al [26], in which the abundant lysosomal enzyme, N-acetyl-ß-D-glucosaminidase (ß-NAG), was measured in the cytosol following MP treatment. Saponin, a known cholesterol-complex forming agent, was utilized to selectively permeabilize cell membranes by targeting membrane-bound cholesterol, which is 5 to 17 times more abundant in cell plasma membrane compared to other organelle membrane [40]. Using a buffer containing an optimized concentration of

saponin, cellular membranes were permeabilized and cytosolic contents were extracted while maintaining the integrity of the intracellular organelles, as previously described in other studies [26, 27]. A branched polycationic polymer, polyethylemine (PEI; 25kDa) was used as a positive control since previous studies have demonstrated PEI's ability to induce endo/lysosomal escape [41, 42]. Following 1 day treatment with fast-degrading Ace-DEX MPs (26% CAC blank MPs), the release of ß-NAG was observed at 16% of total ß-NAG enzyme release, as normalized to complete cell lysis by Triton X-100 (Figure 7). This was comparable to the 55% CAC Ace-DEX MPs at 1 day post treatment (13% ß-NAG release). At 5 days post treatment, the slow-degrading MPs induced significantly higher ß-NAG enzyme release (16%) compared to the fast-degrading MPs (11%), which is consistent with the release profiles (Supplemental Figure 2A & 2B) and the confocal microscopy results (Figure 6A & 6B). PEI induced the greatest ß-NAG enzyme release (25%) following 10 μg/mL treatment for 1 hour at a concentration that is not cytotoxic to the host cell (data not shown). Complementary to our study, Zhan el al. demonstrated 20% lysosomal release following treatment of MPs consisting of a pH-responsive copolymer, poly (BMA-co-PAA, co-2-diethylamino ethyl methacrylate (DMAEMA)) and PLGA [26]. These studies indicated that Ace-DEX MPs are a tunable drug delivery platform capable of inducing lysosomal leakage to allow delivery of cargos to phagosomal and cytosolic targets.

Possible mechanisms have been proposed for the intracellular delivery and lysosomal escape of cargos directed by polymeric MP platforms, such as Ace-DEX. One potential mechanism suggests the role of increased osmotic pressure caused by the degradation of Ace-DEX MPs in the low pH environment of the lysosome, resulting in lysosomal membrane destabilization [43]. It is thought that when pH-responsive polymeric MPs swell in the low pH environment of the endo/lysosome, more lipids are required to maintain stable vesicular structures. This can result in membrane de-stabilization, as described by Murthy et al., or a "proton sponge effect" caused by pH-buffering of protonable groups [44, 45]. Such mechanisms were demonstrated by Hu et al., in which particle swelling of a pH-responsive polymeric nanoparticle resulted in lysosomal rupture and cytosolic delivery of cargo [46]. Interestingly, the slow-degrading particles resulted in the formation of inflated lysosomal structures (Figure 6B), possibly detailing the ability of Ace-DEX MPs at inducing lysosomal rupture by membrane destabilization. Although a viable mechanism, further studies are warranted to determine the buffering and swelling capacity of Ace-DEX MPs at low pH environments to fully access this hypothesis.

In vivo biodistribution of ICG encapsulated Ace-DEX MPs

In the current study, systemic delivery of Ace-DEX MPs was evaluated using a model fluorophore, indocyanine green (ICG), an FDA-approved near-infrared (NIR) imaging agent that has greater optical properties resulting in low background [47]. While no soluble ICG was used in the experiments presented here, it is well documented that soluble ICG is lipophilic and has a very short plasma half-life [48]. Thus, any ICG present within organs after a few hours is due to the sustained delivery of ICG/MPs.

ICG/MPs were administered via intranasal (i.n.), intravenous (i.v.), and intraperitoneal (i.p.) routes at 0.5 mg/kg in mice and organs were evaluated for ICG fluorescence in the liver,

spleen, kidneys, heart, lung, superficial cervical and inguinal lymph nodes (SCLN and ILN, respectively) at set time-points out to 240 hours (Figure 8). As evident by the varying kinetics, trafficking of ICG/MPs was clearly dependent upon the route of administration. The greatest accumulation, as observed by fluorescent intensity and duration, in all organs evaluated was demonstrated following i.n. administration (Figure 8A), with a large quantity of ICG in the liver, kidney and lung, with comparably smaller quantities observed in the SCLN and ILN. ICG persisted in all organs out to 120 hours, and in the liver, kidney and lung, remained out to 240 hours post administration. A steady decline over the study period was observed in all organs. The ability for Ace-DEX MPs to deposit in multiple organs is crucial for inhalational infections caused by pathogens such as *F. tularensis,* which have the ability to spread and infect multiple organs at high efficiency and would require the presence of AR-12 within other organs for successful treatment. Interestingly, the tissue accumulation of Ace-DEX particles seen via i.n. administration is far greater than that reported for PLGA, which only distributed throughout the lungs and bladder over a period of 11 days when given i.n. [49]. Additionally, Ace-DEX MPs demonstrated longer retention compared to ICG-labeled liposomes, which exhibited a decrease in fluorescent intensity, as observed in live-animal imaging, 48 hours post pulmonary administration [50].

Intravenous administration resulted in large quantities of ICG detectable in most organs directly after administration; however, within 6 hours, log reduction is observed, indicating minimal accumulation (Figure 8B). Persistence out to 48 hours was observed in all organs except the lymph nodes, demonstrating extended kinetic properties of Ace-DEX MPs superior to other polymeric delivery platforms. Other studies report that PLGA particles are cleared very rapidly unless modified with polyethylene glycol (PEG), which could indicate a possible solution for the somewhat rapid release seen with Ace-DEX MPs administered in this route [51]. PEGylated liposomal ICG particles also demonstrated mediocre biodistribution kinetics, with a rapid decrease in fluorescent intensities observed in the liver, heart, and kidney 4 hours post administration in CD-1 mice [52].

For i.p. administration (Figure 8C), the largest deposition was in the liver, kidneys, and spleen; however, after three hours, there was a very large reduction of ICG in all organs. Greater accumulation of ICG was observed in the ILN compared to the SCLN; however, log-fold reduction following 3 hours does not indicate an ideal route for extended release kinetics. Similarly, PLGA MPs administered by i.p. did not exhibit high levels of organ deposition, which could indicate this route of administration is not ideal for sustained release of microparticulate vehicles within organs [51].

These trafficking experiments also demonstrate that the differences in sterilization-induced AR-12 release observed after 2.5 weeks (Figure 3) would likely be of little consequence because minimal particle loads were left within organs after 2.5 weeks.

MTD of AR-12/MPs

Previous studies determined that sustained delivery and controlled release of AR-12 from Ace-DEX MPs led to reduced cytotoxicity *in vitro* [4]; however, the toxicity reduction *in vivo* has not previously been explored. Our previous work utilized AR-12/MPs at 2% initial weight loading to deliver AR-12, however, a higher drug-to-excipient ratio was used in the

current study to determine a maximum tolerated dose (MTD) [4, 20, 29]. We were able to increase AR-12 loading up to 20% initial weight loading without a significant decrease in the EE (Table 1). Importantly, AR-12/MPs formulated with EA at 20% initial weight yielded a much higher EE compared to an FDA-approved long-acting injectable formulation with PLGA (Risperdal Consta; Janssen), with similar initial weight loading [53].

The MTD of AR-12/MPs was determined following administration by three routes: i.n, i.v., and i.p.. Following i.n. delivery of AR-12, either soluble or encapsulated, a clear advantage was observed by AR-12/MPs, with an 8-fold increase in the MTD over the soluble AR-12 treatment (Table 2). The toxicity resulting from i.n. administration of AR-12/MPs and the Blank MPs is potentially due to the physical blockage of the airways within nose and lungs, which would significantly limit the mouse's ability to breathe. The higher MTD observed by AR-12/MPs was likely due to phagocyte-directed uptake of MPs, allowing for decreased AR-12 concentrations directly contacting lung milieu. Additionally, the AR-12/MPs that are not phagocytosed immediately within the lungs will slowly release AR-12 over a period of weeks rather than the bolus administration of soluble AR-12 and thus, the concentrations of AR-12 that interact with all lung tissues are far larger for the soluble administration. Thus, this is likely why AR-12/MPs administered via the i.n.route led to enhanced survival with respect to soluble AR-12 following *F. tularensis* infection [29]. Importantly, i.n. administration of drug formulations is simple and painless, providing an additional benefit for treatment of infections that reside in mucosal tissues such as the lungs.

For i.v. delivery, there was a marginal advantage to using AR-12/MPs over soluble AR-12, as the MTD was only increased by 1.5-fold (Table 2). The Blank MP control demonstrated an MTD much higher than the AR-12/MPs, and thus it can be assumed that the MTD is drug-related. In preclinical testing and the phase I clinical trials conducted with soluble AR-12 as a cancer therapy, cardiac toxicity was noted as being one of the dangers of AR-12 [54]. Currently, we observed accumulation of ICG/MPs in the heart and persistence out to 48 hours post injection (Figure 8B). Therefore, it is possible that the toxicity seen via this route at 30 mg/kg is due to cardiac toxicity and thus encapsulation of AR-12 does not result in a high degree of toxicity mitigation.

Contrary to i.n. and i.v. routes, the MTD following delivery to the i.p. space resulted in no benefit of encapsulating AR-12 as the maximum amount of AR-12/MPs that was possible to administer was 80 mg AR-12/kg, which was found to be the limit of particle suspendability (1100 mg/kg) (Table 2). For cancer treatment, the intraperitoneal space is seen as a very robust compartment with only a small number of drug-related adverse events observed and thus, it is not surprising that this route was able to tolerate the highest dose of AR-12 [55].

Conclusion

Previous studies have demonstrated that Ace-DEX MPs facilitate delivery of the putative host-directed therapeutic AR-12 to clear intracellular infections within phagocytes, without the resistance-based complications of pathogen-directed therapeutics [4, 20]. To advance these findings, the current study succeeded at improving the formulation characteristics (EE, release kinetics, and manufacturability) of Ace-DEX encapsulated AR-12. Increasing drug

loading efficiency allows for streamlined scale-up for clinical formulation. Moreover, it was discovered that Ace-DEX MPs can release their cargo and escape the lysosomal compartment very quickly following phagocyte internalization, which is advantageous for a host-directed drug delivery carrier targeting pathogens that are both cytosolic or vesicular-bound. Systemic delivery and increased tissue-specific accumulation via various routes of administration highlight the ability of Ace-DEX MPs to deliver drugs to many organs including the lungs, liver, spleen, and lymph nodes. Organ distribution is an important aspect in evaluating the feasibility of a drug delivery carrier, specifically for treatment of intercellular pathogens such as *F. tularensis* and *S.* Typhi in which the route of infection may dictate the optimal route of therapy. Furthermore, encapsulation in the controlled release Ace-DEX vehicle protected against the toxic effects of soluble AR-12, likely due to increased intracellular delivery of the drug with decreased off-target effects. Coupling these traits with the dose sparing capabilities of Ace-DEX MPs, controlled release and extended biodistribution are some of the most beneficial and desirable traits of new formulated therapies due to a reduction in costs and toxic side effects [56]. Taken together, Ace-DEX MPs represent an advantageous drug delivery system that can be tuned for intracellular delivery and can be used via multiple delivery routes for treatment of intracellular pathogens.

Supplementary Material

Refer to Web version on PubMed Central for supplementary material.

Acknowledgements

References

1. Collier MA; Gallovic MD; Peine KJ; Duong AD; Bachelder EM; Gunn JS; Schlesinger LS; Ainslie KM Delivery of host cell-directed therapeutics for intracellular pathogen clearance. Expert Rev Anti Infect Ther 2013, 11, (11), 1225–35. [PubMed: 24134600]

2. Coburn B; Grassl GA; Finlay BB Salmonella, the host and disease: a brief review. Immunology and cell biology 2007, 85, (2), 112–8. [PubMed: 17146467]

3. Gupta G; Oghumu S; Satoskar AR Mechanisms of immune evasion in leishmaniasis. Advances in applied microbiology 2013, 82, 155–84. [PubMed: 23415155]

4. Hoang KV; Borteh HM; Rajaram MV; Peine KJ; Curry H; Collier MA; Homsy ML; Bachelder EM; Gunn JS; Schlesinger LS; Ainslie KM Acetalated dextran encapsulated AR-12 as a host-directed therapy to control Salmonella infection. Int J Pharm 2014, 477, (1–2), 334–43. [PubMed: 25447826]

5. Chiu HC; Kulp SK; Soni S; Wang D; Gunn JS; Schlesinger LS; Chen CS Eradication of intracellular Salmonella enterica serovar Typhimurium with a smallmolecule, host cell-directed agent. Antimicrob Agents Chemother 2009, 53, (12), 5236–44. [PubMed: 19805568]

6. Chiu HC; Yang J; Soni S; Kulp SK; Gunn JS; Schlesinger LS; Chen CS Pharmacological exploitation of an off-target antibacterial effect of the cyclooxygenase-2 inhibitor celecoxib against Francisella tularensis. Antimicrob Agents Chemother 2009, 53, (7), 2998–3002. [PubMed: 19398640]

7. Chiu HC; Soni S; Kulp SK; Curry H; Wang D; Gunn JS; Schlesinger LS; Chen CS Eradication of intracellular Francisella tularensis in THP-1 human macrophages with a novel autophagy inducing agent. J Biomed Sci 2009, 16, 110. [PubMed: 20003180]

8. Chen HH; Chen CC; Lin YS; Chang PC; Lu ZY; Lin CF; Chen CL; Chang CP AR-12 suppresses dengue virus replication by down-regulation of PI3K/AKT and GRP78. Antiviral Res 2017, 142, 158–168. [PubMed: 28238876]

9. Booth L; Roberts JL; Ecroyd H; Tritsch SR; Bavari S; Reid SP; Proniuk S; Zukiwski A; Jacob A; Sepulveda CS; Giovannoni F; Garcia CC; Damonte E; Gonzalez-Gallego J; Tunon MJ; Dent P AR-12 Inhibits Multiple Chaperones Concomitant With Stimulating Autophagosome Formation Collectively Preventing Virus Replication. J Cell Physiol 2016, 231, (10), 2286–302. [PubMed: 27187154]

10. Abdulrahman BA; Abdelaziz D; Thapa S; Lu L; Jain S; Gilch S; Proniuk S; Zukiwski A; Schatzl HM The celecoxib derivatives AR-12 and AR-14 induce autophagy and clear prion-infected cells from prions. Sci Rep 2017, 7, (1), 17565. [PubMed: 29242534]

11. Bachelder EM; Pino EN; Ainslie KM Acetalated Dextran: A Tunable and Acid-Labile Biopolymer with Facile Synthesis and a Range of Applications. Chem Rev 2017, 117, (3), 1915–1926. [PubMed: 28032507]

12. Bachelder EM; Beaudette TT; Broaders KE; Dashe J; Frechet JM Acetal-derivatized dextran: an acid-responsive biodegradable material for therapeutic applications. J Am Chem Soc 2008, 130, (32), 10494–5. [PubMed: 18630909]

13. Kauffman KJ; Do C; Sharma S; Gallovic MD; Bachelder EM; Ainslie KM Synthesis and characterization of acetalated dextran polymer and microparticles with ethanol as a degradation product. ACS Appl Mater Interfaces 2012, 4, (8), 4149–55. [PubMed: 22833690]

14. Suarez S; Grover GN; Braden RL; Christman KL; Almutairi A Tunable protein release from acetalated dextran microparticles: a platform for delivery of protein therapeutics to the heart post-MI. Biomacromolecules 2013, 14, (11), 3927–35. [PubMed: 24053580]

15. Chen N; Collier MA; Gallovic MD; Collins GC; Sanchez CC; Fernandes EQ; Bachelder EM; Ainslie KM Degradation of acetalated dextran can be broadly tuned based on cyclic acetal coverage and molecular weight. Int J Pharm 2016, 512, (1), 147–57. [PubMed: 27543351]

16. Zolnik BS; Burgess DJ Effect of acidic pH on PLGA microsphere degradation and release. Journal of controlled release : official journal of the Controlled Release Society 2007, 122, (3), 338–44. [PubMed: 17644208]

17. Liu Y; Ghassemi AH; Hennink WE; Schwendeman SP The microclimate pH in poly(D,L-lactide-co-hydroxymethyl glycolide) microspheres during biodegradation. Biomaterials 2012, 33, (30), 7584–93. [PubMed: 22819499]

18. Fu K; Pack DW; Klibanov AM; Langer R Visual evidence of acidic environment within degrading poly(lactic-co-glycolic acid) (PLGA) microspheres. Pharm Res 2000, 17, (1), 100–6. [PubMed: 10714616]

19. Kanthamneni N; Sharma S; Meenach SA; Billet B; Zhao JC; Bachelder EM; Ainslie KM Enhanced stability of horseradish peroxidase encapsulated in acetalated dextran microparticles stored outside cold chain conditions. International journal of pharmaceutics 2012, 431, (1–2), 101–10. [PubMed: 22548844]

20. Collier MA; Peine KJ; Gautam S; Oghumu S; Varikuti S; Borteh H; Papenfuss TL; Satoskar AR; Bachelder EM; Ainslie KM Host-mediated Leishmania donovani treatment using AR-12 encapsulated in acetalated dextran microparticles. International journal of pharmaceutics 2016, 499, (1–2), 186–94. [PubMed: 26768723]

21. Munsell EV; Ross NL; Sullivan MO Journey to the Center of the Cell: Current Nanocarrier Design Strategies Targeting Biopharmaceuticals to the Cytoplasm and Nucleus. Curr Pharm Des 2016, 22, (9), 1227–44. [PubMed: 26675220]

22. Schulze K; Ebensen T; Riese P; Prochnow B; Lehr CM; Guzman CA New Horizons in the Development of Novel Needle-Free Immunization Strategies to Increase Vaccination Efficacy. Curr Top Microbiol Immunol 2016, 398, 207–234. [PubMed: 27370343]

23. Shakya AK; Kumar A; Nandakumar KS Adjuvant properties of a biocompatible thermo-responsive polymer of N-isopropylacrylamide in autoimmunity and arthritis. J R Soc Interface 2011, 8, (65), 1748–59. [PubMed: 21543351]

24. Gallovic MD; Bandyopadhyay S; Borteh H; Montjoy DG; Collier MA; Peine KJ; Wyslouzil BE; Bachelder EM; Ainslie KM Microparticles formulated from a family of novel silylated polysaccharides demonstrate inherent immunostimulatory properties and tunable hydrolytic degradability. 2016.

25. Bolte S; Cordelieres FP A guided tour into subcellular colocalization analysis in light microscopy. J Microsc 2006, 224, (Pt 3), 213–32. [PubMed: 17210054]

26. Zhan X; Tran KK; Wang L; Shen H Controlled Endolysosomal Release of Agents by pH-responsive Polymer Blend Particles. Pharm Res 2015, 32, (7), 2280–91. [PubMed: 25592550]

27. Foghsgaard L; Wissing D; Mauch D; Lademann U; Bastholm L; Boes M; Elling F; Leist M; Jaattela M Cathepsin B acts as a dominant execution protease in tumor cell apoptosis induced by tumor necrosis factor. J Cell Biol 2001, 153, (5), 999–1010. [PubMed: 11381085]

28. Le Tourneau C; Lee JJ; Siu LL Dose escalation methods in phase I cancer clinical trials. Journal of the National Cancer Institute 2009, 101, (10), 708–20. [PubMed: 19436029]

29. Hoang KV; Curry H; Collier MA; Borteh H; Bachelder EM; Schlesinger LS; Gunn JS; Ainslie KM Needle-Free Delivery of Acetalated Dextran-Encapsulated AR-12 Protects Mice from Francisella tularensis Lethal Challenge. Antimicrob Agents Chemother 2016, 60, (4), 2052–62. [PubMed: 26787696]

30. Yeo Y; Park K Control of encapsulation efficiency and initial burst in polymeric microparticle systems. Arch Pharm Res 2004, 27, (1), 1–12. [PubMed: 14969330]

31. Xu L; Anchordoquy T Drug delivery trends in clinical trials and translational medicine: challenges and opportunities in the delivery of nucleic acid-based therapeutics. Journal of pharmaceutical sciences 2011, 100, (1), 38–52. [PubMed: 20575003]

32. Abuhanoglu G; Ozer AY Radiation sterilization of new drug delivery systems. Interventional medicine & applied science 2014, 6, (2), 51–60. [PubMed: 24936306]

33. Pekkarinen T; Hietalal O; Jamsa T; Jalovaara P Gamma irradiation and ethylene oxide in the sterilization of native reindeer bone morphogenetic protein extract. Scandinavian journal of surgery : SJS : official organ for the Finnish Surgical Society and the Scandinavian Surgical Society 2005, 94, (1), 67–70.

34. Junkins R; Gallovic M; Johnson B; Collier M; Watkins-Schulz R; Cheng N; David C; McGee C; Sempowski G; Shterev I; McKinnone K; Bachelder E; Ainslie K; Ting J A robust microparticle platform for a STING-targeted adjuvant that enhances both humoral and cellular immunity during vaccination. Journal of Controlled Release 2017, 21, (270), 1–13.

35. Grandfils C; Flandroy P; Nihant N; Barbette S; Jerome R; Teyssie P; Thibaut A Preparation of poly (D,L) lactide microspheres by emulsion-solvent evaporation, and their clinical applications as a convenient embolic material. J Biomed Mater Res 1992, 26, (4), 467–79. [PubMed: 1601900]

36. Kohane DS; Tse JY; Yeo Y; Padera R; Shubina M; Langer R Biodegradable polymeric microspheres and nanospheres for drug delivery in the peritoneum. J Biomed Mater Res A 2006, 77, (2), 351–61. [PubMed: 16425240]

37. Dai Z; Ronholm J; Tian Y; Sethi B; Cao X Sterilization techniques for biodegradable scaffolds in tissue engineering applications. Journal of tissue engineering 2016, 7, 2041731416648810. [PubMed: 27247758]

38. Chen N; Johnson MM; Collier MA; Gallovic MD; Bachelder EM; Ainslie KM Tunable degradation of acetalated dextran microparticles enables controlled vaccine adjuvant and antigen delivery to modulate adaptive immune responses. J Control Release 2018, 273, 147–159. [PubMed: 29407676]

39. Blanco E; Shen H; Ferrari M Principles of nanoparticle design for overcoming biological barriers to drug delivery. Nature biotechnology 2015, 33, (9), 941–51.

40. Korn ED Cell membranes: structure and synthesis. Annu Rev Biochem 1969, 38, 263–88. [PubMed: 4896240]

41. Mazzaglia A; Scala A; Sortino G; Zagami R; Zhu Y; Sciortino MT; Pennisi R; Pizzo MM; Neri G; Grassi G; Piperno A Intracellular trafficking and therapeutic outcome of multiwalled carbon nanotubes modified with cyclodextrins and polyethylenimine. Colloids Surf B Biointerfaces 2018, 163, 55–63. [PubMed: 29277018]

42. Shi B; Zheng M; Tao W; Chung R; Jin D; Ghaffari D; Farokhzad OC Challenges in DNA Delivery and Recent Advances in Multifunctional Polymeric DNA Delivery Systems. Biomacromolecules 2017, 18, (8), 2231–2246. [PubMed: 28661127]

43. Huang L Nanoparticles escaping RES and endosome: Challenges for siRNA delivery for cancer therapy. Journal of Nanomaterials 2011.

44. Panyam J; Zhou WZ; Prabha S; Sahoo SK; Labhasetwar V Rapid endo-lysosomal escape of poly(DL-lactide-co-glycolide) nanoparticles: implications for drug and gene delivery. FASEB journal : official publication of the Federation of American Societies for Experimental Biology 2002, 16, (10), 1217–26. [PubMed: 12153989]

45. Murthy N; Robichaud JR; Tirrell DA; Stayton PS; Hoffman AS The design and synthesis of polymers for eukaryotic membrane disruption. J Control Release 1999, 61, (1–2), 137–43. [PubMed: 10469910]

46. Hu Y; Litwin T; Nagaraja AR; Kwong B; Katz J; Watson N; Irvine DJ Cytosolic delivery of membrane-impermeable molecules in dendritic cells using pH-responsive core-shell nanoparticles. Nano Lett 2007, 7, (10), 3056–64. [PubMed: 17887715]

47. De Grand AM; Lomnes SJ; Lee DS; Pietrzykowski M; Ohnishi S; Morgan TG; Gogbashian A; Laurence RG; Frangioni JV Tissue-like phantoms for near-infrared fluorescence imaging system assessment and the training of surgeons. Journal of biomedical optics 2006, 11, (1), 014007. [PubMed: 16526884]

48. Ebert B; Riefke B; Sukowski U; Licha K Cyanine dyes as contrast agents for near-infrared imaging in vivo: acute tolerance, pharmacokinetics, and fluorescence imaging. Journal of biomedical optics 2011, 16, (6), 066003. [PubMed: 21721804]

49. Vij N; Min T; Marasigan R; Belcher CN; Mazur S; Ding H; Yong KT; Roy I Development of PEGylated PLGA nanoparticle for controlled and sustained drug delivery in cystic fibrosis. J Nanobiotechnology 2010, 8, 22. [PubMed: 20868490]

50. Murata M; Tahara K; Takeuchi H Real-time in vivo imaging of surface-modified liposomes to evaluate their behavior after pulmonary administration. Eur J Pharm Biopharm 2014, 86, (1), 115–9. [PubMed: 24055689]

51. Liu R; Colby AH; Gilmore D; Schulz M; Zeng J; Padera RF; Shirihai O; Grinstaff MW; Colson YL Nanoparticle tumor localization, disruption of autophagosomal trafficking, and prolonged drug delivery improve survival in peritoneal mesothelioma. Biomaterials 2016, 102, 175–86. [PubMed: 27343465]

52. Beziere N; Lozano N; Nunes A; Salichs J; Queiros D; Kostarelos K; Ntziachristos V Dynamic imaging of PEGylated indocyanine green (ICG) liposomes within the tumor microenvironment using multi-spectral optoacoustic tomography (MSOT). Biomaterials 2015, 37, 415–24. [PubMed: 25453969]

53. Sajeev Kumar PB; Pandey RS; Thirthali J; Siva Kumar PT; Naveen Kumar C A Comparative Study Of Short Term Efficacy Of Aripiprazole And Risperidone In Schizophrenia. Current neuropharmacology 2017.

54. Therapeutics, A., Study of AR-12 (2-Amino-N-[4-[5-(2 Phenanthrenyl)-3-(Trifluoromethyl)-1H-pyrazol-1-yl] Phenyl]-Acetamide) in Adult Patients With Advanced or Recurrent Solid Tumors or Lymphoma. ClinicalTrials.gov: 2014.

55. Yang S; Feng R; Pan ZC; Jiang T; Xu Q; Chen Q A Comparison of Intravenous plus Intraperitoneal Chemotherapy with Intravenous Chemotherapy Alone for the Treatment of Gastric Cancer: A Meta-Analysis. Scientific reports 2015, 5, 12538. [PubMed: 26220081]

56. Singh OP; Sundar S Immunotherapy and targeted therapies in treatment of visceral leishmaniasis: current status and future prospects. Frontiers in immunology 2014, 5, 296. [PubMed: 25183962]
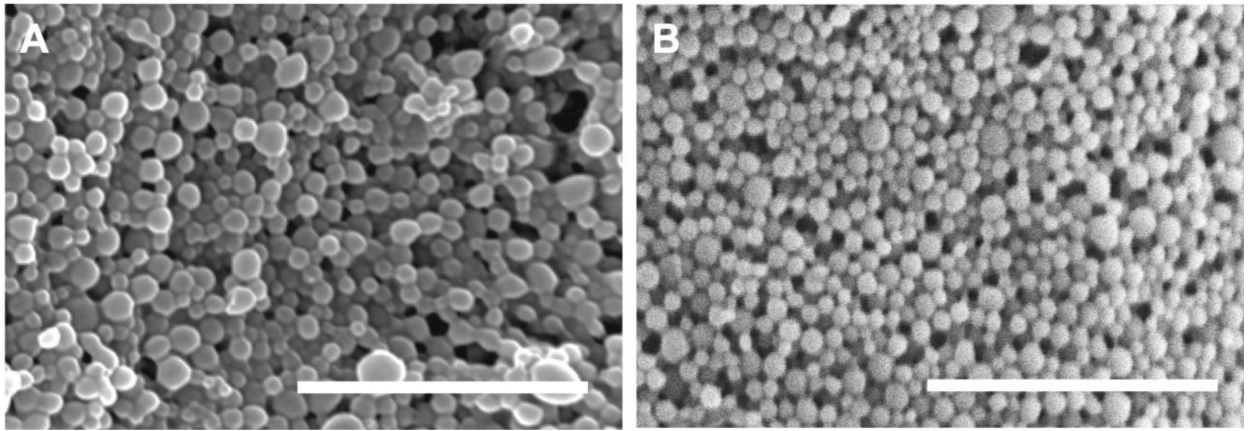
Figure 1. Scanning electron microscopy images of Ace-DEX MPs.
Scanning electron micrographs of Ace-DEX MPs composed of native polymer encapsulating AR-12 (AR12/MPs) by (A) dichloromethane (DCM), or (B) ethyl acetate (EA). Representative image of three independent experiments. Scale bar is 1 μm.
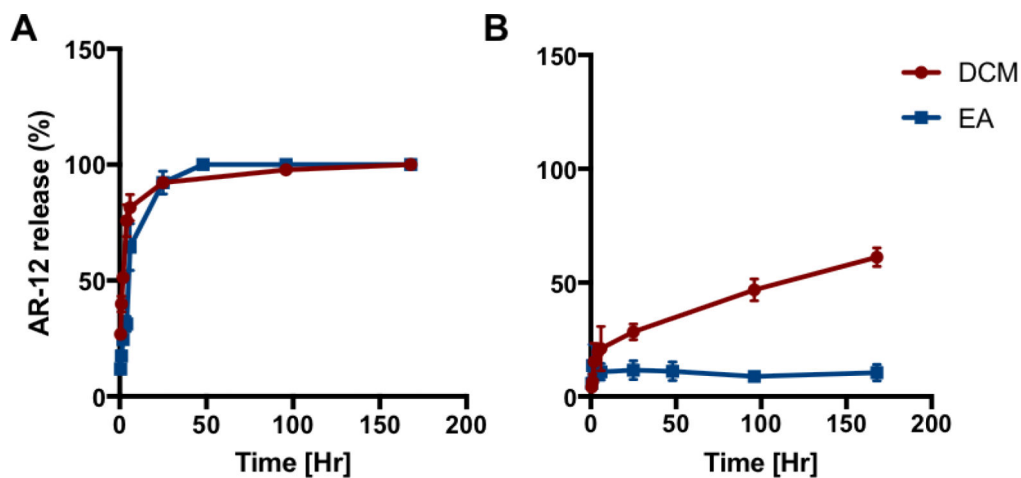
Figure 2. Drug release kinetics of Ace-DEX MPs encapsulating AR-12.
In vitro drug release performed at (A) pH 5 and (B) pH 7.4 of AR-12 encapsulated Ace-DEX MPs fabricated with dichloromethane (DCM; red) or ethyl acetate (EA; blue). Values are reported as mean percent release normalized to the zero time point ± SEM.
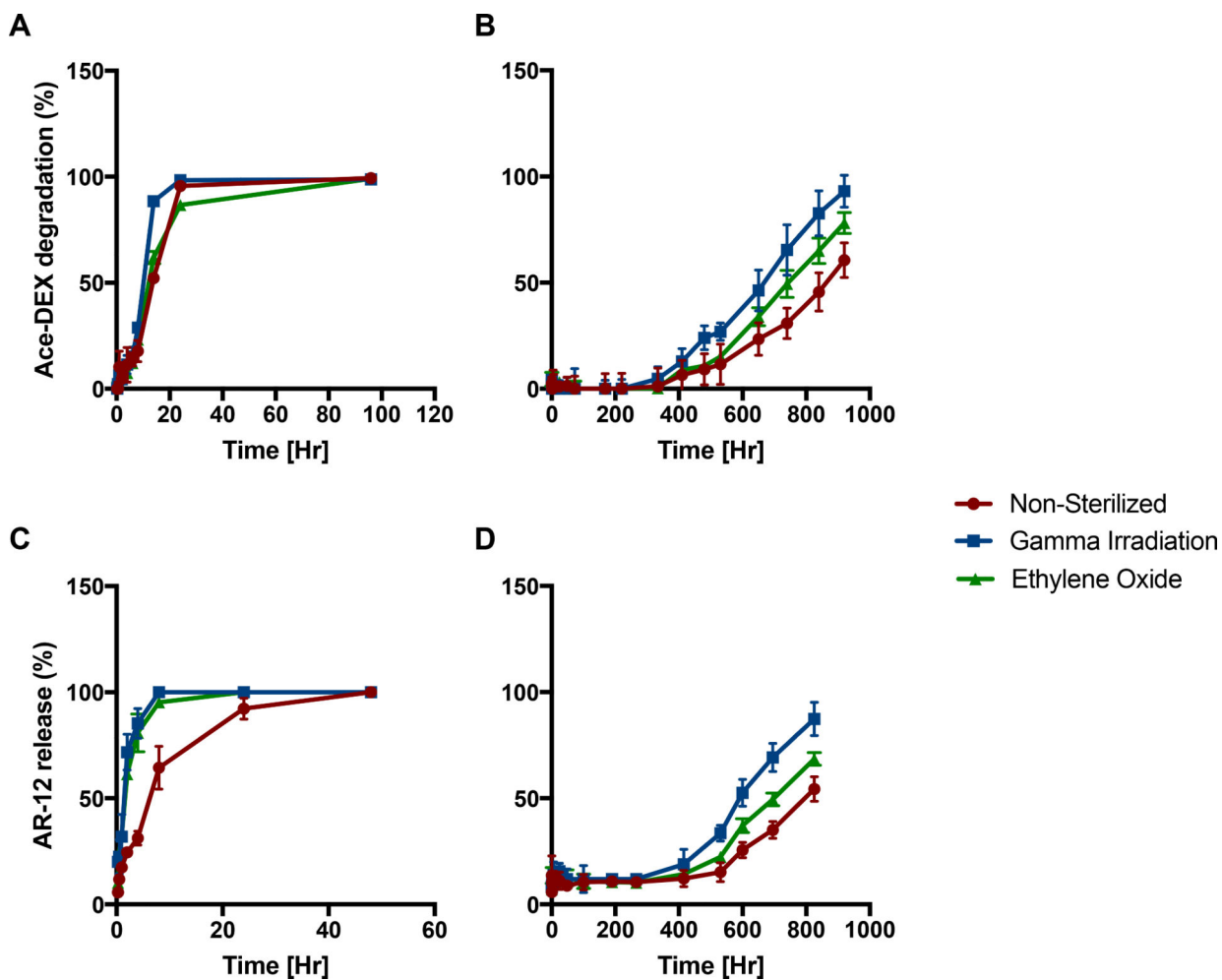
Figure 3. Degradation and AR-12 release profiles of sterilized acetalated dextran microparticles encapsulating AR-12 (AR-12/MPs).

AR-12/MPs non-sterilized, or sterilized by gamma irradiation or ethylene oxide treatment were evaluated for Ace-DEX degradation at (A) pH 5 and (B) pH 7.4. Drug release of AR-12 was evaluated at (C) pH 5 and (D) pH 7.4 Values are reported as mean percent release normalized to time [0] ± SEM ($n = 3$).
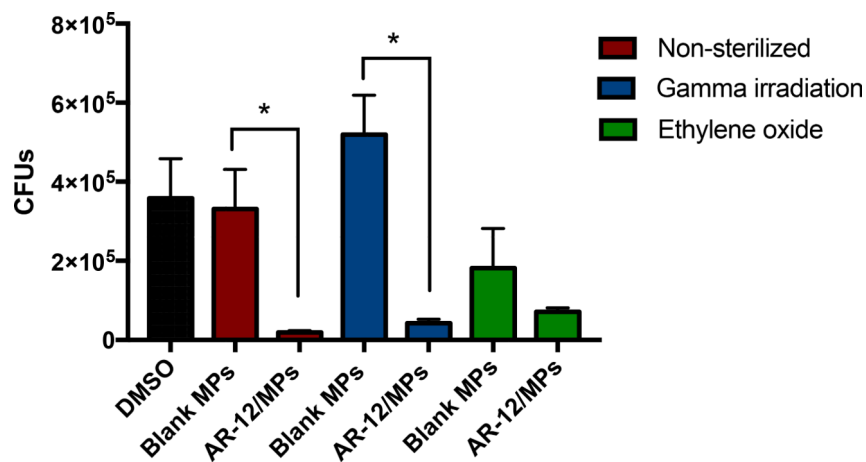
Figure 4. Therapeutic efficacy of sterilized AR-12/MPs against intracellular *Salmonella enterica* Typhi infection.

Human monocyte derived macrophages (hMDMs) were treated with acetalated dextran microparticles encapsulating AR-12 (AR-12/MPs; 5 μM) or respective blank acetalated dextran microparticles (Blank MPs; 144 μg), either non-sterilized (red bars), gamma irradiated (blue bars), or ethylene oxide treated (green bars). * indicates significance of p <0.05. Data are presented as mean ± standard deviation of three independent experiments.
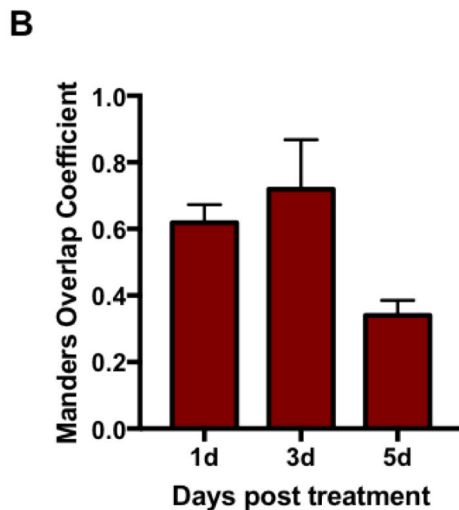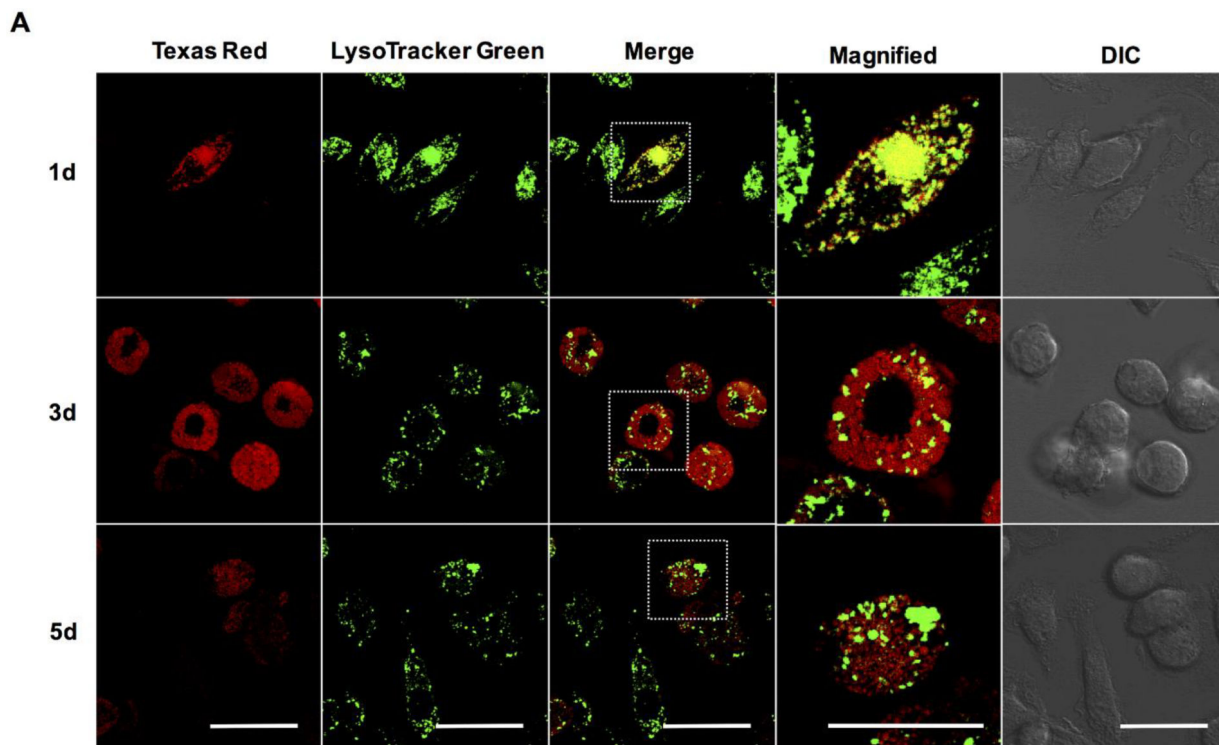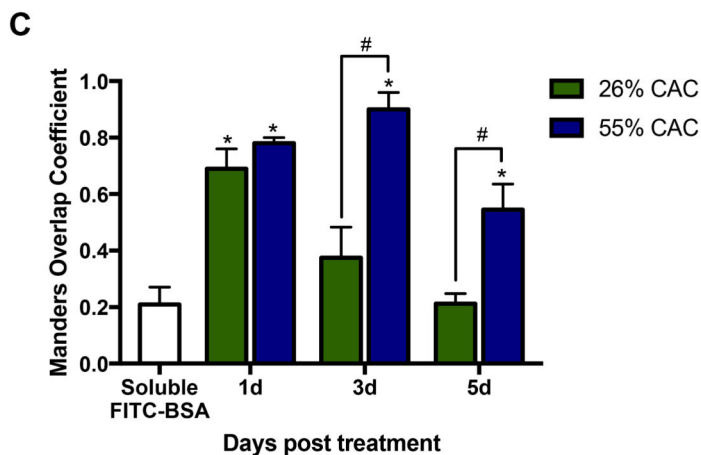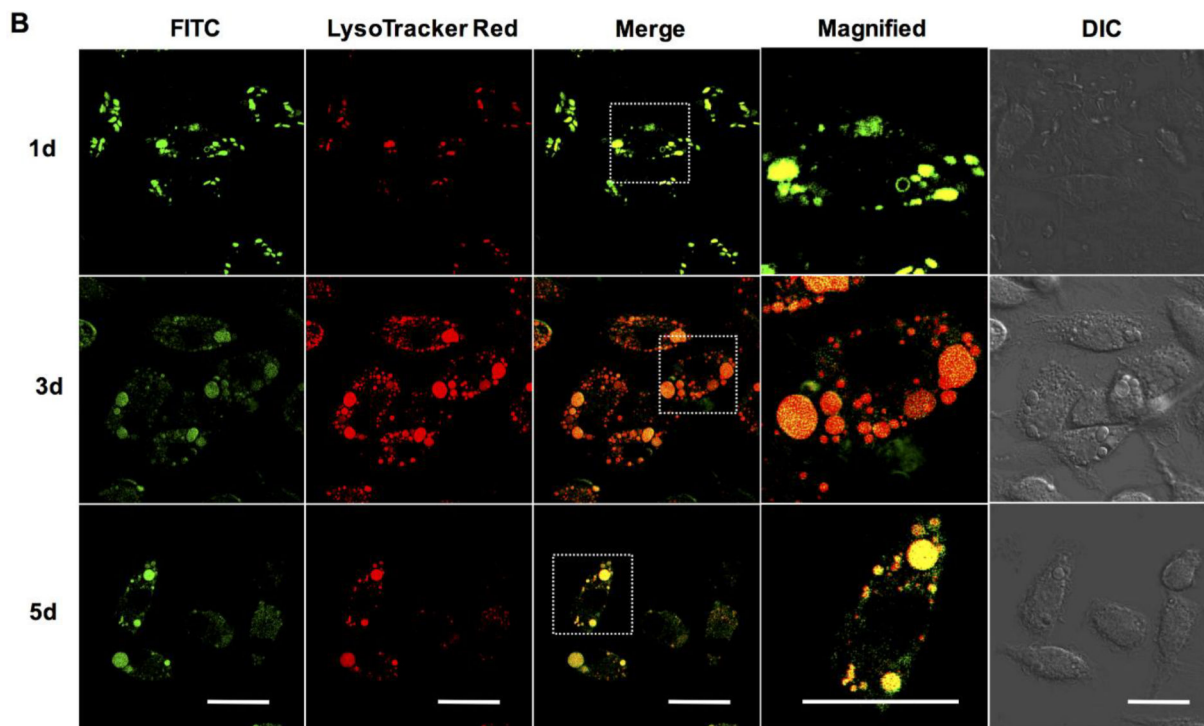
Figure 5. Confocal microscopic analysis of time-dependent Texas Red/Ace-DEX MPs co-localization to the lysosomes and cytosolic escape.

(A) Ace-DEX MPs composed of Texas Red-conjugated Ace-DEX were delivered to bone marrow-derived macrophages at set time points, followed by live cell imaging using laser scanning confocal microscopy (40× oil immersion). Red: Texas Red microparticles, green: LysoTracker Green dye. Representative image of three independent experiments. Scale bar is 10 μm. B) Co-localization was quantitatively measured by computing co-localization coefficients (Manders Overlap) using Image J and the plug-in JaCop. Values are reported as mean ± SEM.
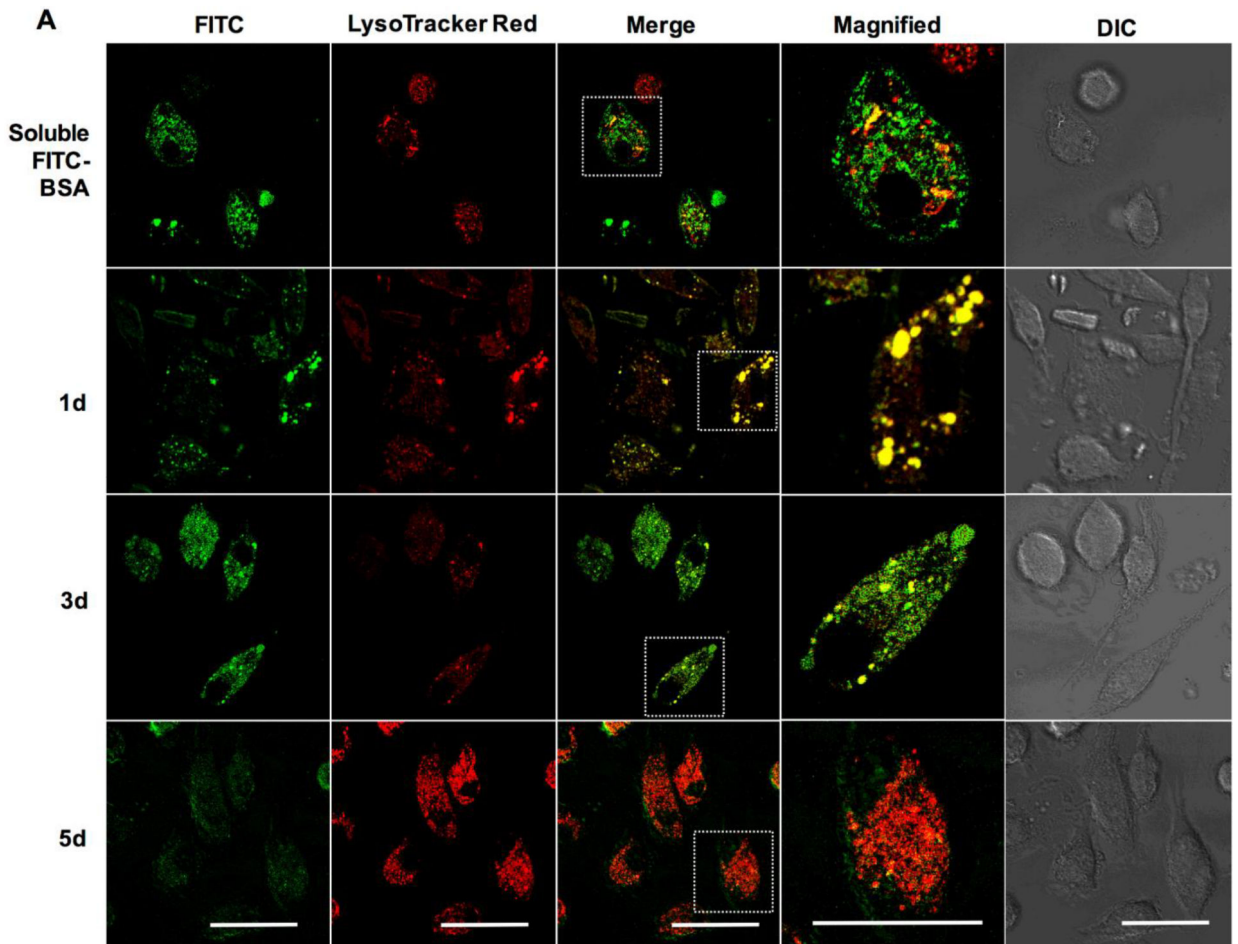
Figure 6. Time-dependent confocal microscopic analysis of fast- and slow-degrading FITC-BSA encapsulated Ace-DEX MPs co-localized to lysosomes.

Ace-DEX MPs composed of native Ace-DEX at (A) 26% cyclic acetal coverage (CAC) and (B) 55% CAC encapsulating FITC-BSA were delivered to bone marrow-derived macrophages at set time points, followed by live cell imaging using laser scanning confocal microscopy (40× oil immersion). Green: FITC-BSA, red: LysoTracker Red dye. Representative image of three independent experiments. Scale bar is 10 μm. (C) Using confocal images, co-localization was quantitatively measured by computing co-localization coefficients (Manders Overlap) using Image J and the plug-in JaCop for 26% (white bar) and 55% CAC (grey bar) Ace-DEX MPs, respectively. Values are reported as mean ± SEM.
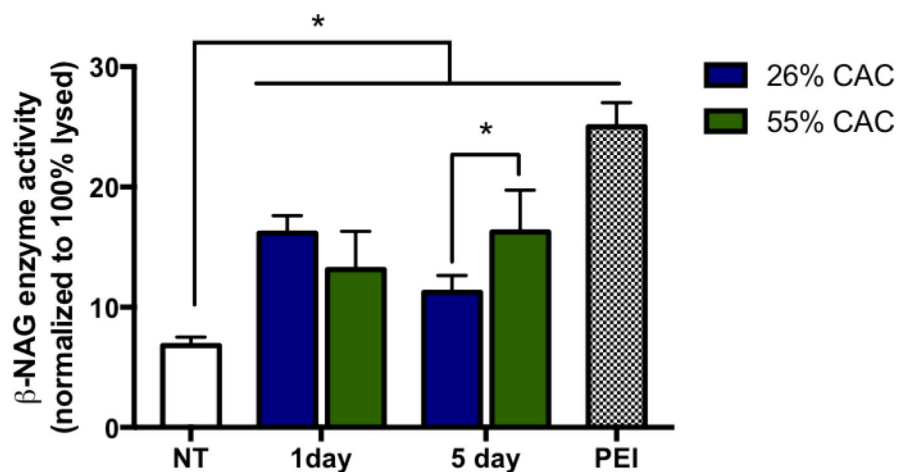
* indicates significance at $p < 0.05$ compared to non-treated control groups and [#] indicates significance between 26% and 55% CAC MPs.

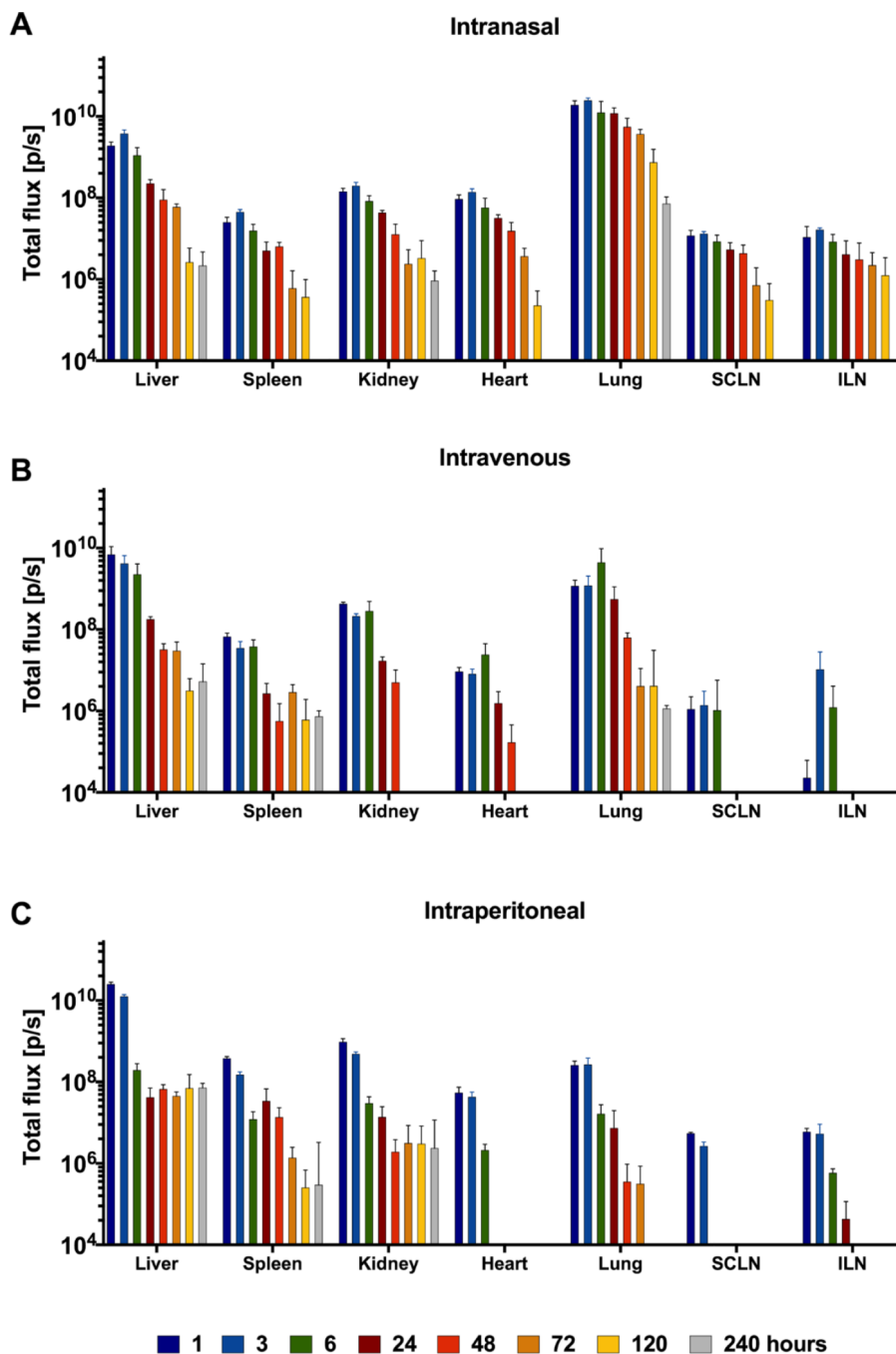**Figure 7. Time-dependent release of endo/lysosomal enzyme, N-acetyl-β-D-glucosaminidase (β-NAG), directed by Ace-DEX MPs and PEI.**

BMDMs were treated with 26% CAC (blue bar) or 55% CAC (green bar) Ace-DEX MPs (0.5 mg/mL) for 1 and 5 days, respectively. PEI (10 µg) treatment for 1 hour was used as a positive control (checkered bar). Cytosolic β-NAG activity was measured with the N-acetyl-β-D-glucosaminidase assay and expressed as enzyme activity normalized to Triton 100-X lysed cells (100% lysed). Values are reported as mean ± SEM. * indicates significance of $p < 0.05$.

A Intranasal

B Intravenous

C Intraperitoneal

Legend: 1 | 3 | 6 | 24 | 48 | 72 | 120 | 240 hours

Figure 8: *In vivo* particle trafficking of ICG Ace-DEX microparticles (ICG/MPs).
Mice were injected with 0.5 mg/kg of ICG MPs via (A) intranasal, (B) intravenous, and (C) intraperitoneal administration routes. At set time points, accumulation was measured in the liver, spleen, kidney, heart, lungs, superficial cervical lymph nodes (SCLN), and inguinal lymph nodes (ILN) using IVIS. Values are reported as mean total flux [p/s] ± SEM (n=4).

Table 1.

Characterization of acetalated dextran microparticles (Ace-DEX MPs) encapsulating AR-12/MPs formulated with dichloromethane (DCM) or ethyl acetate (EA).

Data are presented as mean ± standard deviation (n=3)

	DCM	EA	
Initial Weight Loading (% w/w)	2%	2%	20%
AR-12 Encapsulation Efficiency (%)	31.5 ± 1.8	80.3 ± 2.5	81.5 ± 4.6

Table 2:

Maximum tolerated dose of blank acetalated dextran microparticles (Blank MPs), acetalated dextran microparticles encapsulating AR-12 (AR-12/MPs) and soluble AR-12. Sol = soluble

	Route								
	Intranasal			Intravenous			Intraperitoneal		
Formulation	Blank MPs	AR-12/MPs	Sol AR-12	Blank MPs	AR-12/MPs	Sol AR-12	Blank MPs	AR-12/MPs	Sol AR-12
Maximum tolerated AR-12 dose [mg/kg]	-	24	3	-	30	20	-	80 [*]	80
Ace-DEX MPs [mg/kg]	170	140	-	470	190	-	1100 [*]	1100 [*]	-

[*] Maximum particle suspendability [mg/kg]